Positrons and Antiprotons in Galactic Cosmic Rays

R. Cowsik

Physics Department and McDonnell Center for the Space Sciences, Washington University in St. Louis, St. Louis, Missouri 63130; email: cowsik@wustl.edu

Annu. Rev. Nucl. Part. Sci. 2016. 66:297–319

First published online as a Review in Advance on July 6, 2016

The *Annual Review of Nuclear and Particle Science* is online at nucl.annualreviews.org

This article's doi: 10.1146/annurev-nucl-102115-044851

Keywords

positrons, antiprotons, cosmic rays, dark matter, Galactic sources

Abstract

I consider the impact of recent measurements of positron and antiproton spectra in cosmic rays on our understanding of the origins and propagation of cosmic rays, as well as on the annihilation and decay characteristics of particles of Galactic dark matter, from the perspective of current models postulating energy-dependent leakage of cosmic rays from the Galaxy and of the nested leaky-box model, in which the leakage from the Galaxy is independent of energy. The nested leaky-box model provides a straightforward and consistent explanation of the observed spectral intensities, and finds no compelling need for a contribution from the annihilation or decay of Galactic dark matter. Improved observations and modeling efforts are needed to probe the properties of dark matter deeply enough to be significant to particle physics and cosmology.

Contents

1. INTRODUCTION

The origin and propagation of cosmic rays, and the nature and properties of dark matter in our Galaxy, are outstanding questions in the field of astroparticle physics. During the last several years, the space missions PAMELA and AMS have measured the fluxes of positrons and antiprotons with unprecedented energy coverage, extending up to almost 1,000 GeV, and have helped us address these questions. Details of these measurements, carried out with very high statistical precision and wide energy coverage, have been presented by Ting (1).

The fields of cosmic-ray and dark matter research began with momentous discoveries in the first half of the twentieth century. In 1912, Hess's (2) observation that the ionization rate increases as one moves up in the Earth's atmosphere led to the discovery of cosmic rays, and in 1933, Zwicky's (3) observation that the random motions of galaxies in the Coma Cluster were too large to be bound to the cluster by the gravitational forces exerted only by visible matter led to the discovery of dark matter. Many excellent articles, including several in earlier volumes of Annual Reviews journals, have comprehensively covered these two topics (4–12). The main purpose of this review is to focus on recent observations on positrons and antiprotons in cosmic rays, and to discuss their implications to the fields of cosmic rays and dark matter in a self-contained manner and with minimal formalism or computational complexity. This review also emphasizes the discrete nature of the sources of cosmic rays in the Galaxy, which helps us understand some of the puzzling aspects of the observations.

1.1. Cosmic-Ray Astrophysics: The Beginnings

The advent of the space age in the 1960s enabled measurements of cosmic-ray spectra and composition down to ~100 MeV per nucleon without the modifications introduced by the Earth's atmosphere. At the same time, researchers realized that the field of cosmic rays would provide insight into high-energy astrophysics in general and nonthermal phenomena in particular. Two

masterly and prescient books on this subject were published, the first by Ginzburg & Syrovatskii (13) in 1964 and the second, with a slightly different emphasis, by Hayakawa (14) in 1969.

The early observations started with a puzzle: The spectral intensities of Li, Be, and B, called the L nuclei, and those of C, N, and O, called the M nuclei, were measured over the energy range from ~100 MeV per nucleon to 3 GeV per nucleon. Because the universal abundances of Li, Be, and B are extremely low, their much higher ratio with respect to C, N, and O in cosmic rays was immediately interpreted as a result of spallation of the latter nuclei during their traversal of interstellar matter following the generation of cosmic rays. The interpretation was that this intervening matter took the form of a slab with sufficient thickness to produce the observed ratio (Li+Be+B)/(C+O) generated by steeply declining spectra of primary nuclei at low energies. No single thickness yielded both the right ratio and the right spectra. To remedy this problem, researchers developed the leaky-box (LB) model, which postulates that cosmic rays injected into the Galactic volume by their sources diffused through the volume and then escaped into the intergalactic space randomly, with an effective time constant τ, irrespective of where and when they were created (15). The broad distribution of path lengths through interstellar matter enabled simultaneous fitting of both the spectra and the ratios with the same value of τ (15, 16). This model was also used to interpret the then-available spectra of cosmic-ray electrons and the newly discovered universal microwave background in order to estimate the value of τ to be approximately 2–3 My (17). As the data accumulated, the LB model was generally adopted to interpret the data (4).

The correspondence between the LB model and models that explicitly use the diffusion equation with boundary conditions assuming that the cosmic-ray density vanishes at the boundary has been discussed by Jones (18) and succinctly summarized by Maurin et al. (19). It is generally recognized that the diffusion term $\nabla \cdot (D\nabla N)$ in the context of partially reflecting boundaries can be approximated by $-N/\tau$, as long as the density and other properties of the diffusion volume are replaced by appropriate average parameters. Following Ginzburg & Syrovatskii (13) and Berezinskii et al. (20), we may write

$$N(\mathbf{r}) = \int q(\mathbf{r}')G(\mathbf{r}, \mathbf{r}')d^3r, \qquad 1.$$

so that the function $G(\mathbf{r}, \mathbf{r}')$ encodes all aspects of propagation and the boundary conditions. In their formulation of the LB model, Cowsik et al. (15) approximated the function $G(\mathbf{r}, \mathbf{r}') \sim G(|\mathbf{r} - \mathbf{r}'|) \sim G(\beta ct)$ and called it the vacuum path-length distribution, in which all the interactions, such as spallation and energy loss, are switched off. Various processes that take place during propagation specific to any particle can later be allowed to modify the function G. Cowsik et al. exemplified this approach with the simplest and most convenient possibility,

$$G \sim \exp(-t/\tau), \qquad 2.$$

or, equivalently, in terms of the grammage, $x = \beta c\rho t$,

$$G \sim \exp(-x/\lambda). \qquad 3.$$

In the early 1970s, these observations were extended to higher energies (up to ~100 GeV per nucleon), which indicated that the ratios of Li, Be, and B to C and O decreased with energy (21–23), necessitating modifications to the simple LB model. Juliusson et al. (21) and Audouze & Cesarsky (24) suggested a straightforward modification wherein the leakage lifetime τ from the Galaxy is a decreasing function of energy, matching the decrease of the B/C ratio:

$$\tau(E) \sim \tau_0 E^{-\delta}, \qquad 4.$$

where $\delta \sim 0.7$. Because the observed spectrum $F(E)$ of primary cosmic rays such as C is given essentially by

$$F(E) = \frac{c}{4\pi} q(E)\tau(E) \sim E^{-2.7}, \quad 5.$$

the injection spectrum $q(E)$ emerging from the sources should be relatively flat:

$$q(E) \sim E^{-(2.7-\delta)}. \quad 6.$$

This energy-dependent leakage (EDL) model proposed by Juliusson et al. (21) and by Audouze & Cesarsky (24) had many attractive features. The relatively flat source spectrum of approximately E^{-2}, necessitated by rapid leakage of cosmic rays at higher energies from the Galaxy, fitted well with the spectrum expected of particles accelerated in high–Mach number shocks (25–28). First, research by Bell (27) and others showed that nearly planar shocks in the expansion of debris from supernova explosions could efficiently transfer a significant fraction of the kinetic energy of the debris into energetic particles in a process similar to first-order Fermi acceleration. Second, the theory of scattering of energetic charged particles in random magnetic fields was being developed (29–31) from the perspective of both laboratory plasmas and cosmic rays propagating in the interstellar medium (ISM). These studies suggested that the diffusion constant had varied with the rigidity of the particles in a way that depended on the spectral density of the inhomogeneities in wave-number space. This theoretical interplay between scattering theory and modeling on one hand and the progressively improving observations of cosmic-ray spectra and composition on the other hand stimulated further development of models with EDL or, equivalently, an energy-dependent diffusion constant.

On the basis of the same data, Cowsik & Wilson (32) and Meneguzzi (33, 34) suggested that cosmic rays may suffer spallation in the matter immediately surrounding the sources, generating secondary nuclei predominantly at lower energies, as higher-energy cosmic rays escape more freely. Cowsik and Wilson argued further that the values of δ in the range ~ 0.5 to ~ 0.7 required to fit the available observations would imply a very short lifetime and rapid streaming of cosmic rays at high energies, leading to unacceptably large anisotropies (35, 36). In the alternate model, they made several assumptions:

1. The Galactic disc was sprinkled randomly with a large number of sources.
2. All cosmic-ray nuclei were accelerated to the same spectral form of $\sim E^{-2.7}$ at high energies.
3. Subsequent to the acceleration process, cosmic rays diffused across a lumpy shell of stellar debris and other material in an energy-dependent fashion, generating the energy-dependent excess of secondary nuclei, such as B, observed at lower energies.
4. Further transport in the general ISM and leakage into the intergalactic medium were nearly independent of the energies of cosmic rays, up to almost $\sim 10^6$ GeV. The spallation in the ISM generated a baseline for the B/C ratio to which the energy-dependent contribution from the sources was added to yield the observed ratios. The energy-independent constant lifetime in the ISM should be sufficient to meet the observed bounds on anisotropy of cosmic rays.
5. During this residence time in the Galaxy, cosmic rays generated secondary nuclei (and, of course, positrons, antiprotons, and others) whose spectra dominate at high energies as the spectra of secondary particles from production in the source regions taper off rapidly at high energies.

For high energies ($E > 1$ GeV per nucleon), where the energy losses due to ionization losses are small and the spallation cross sections are independent of energy, Cowsik & Wilson (32) provided a simple matrix method to calculate the abundances of all nuclei, taking into account interaction effects to all orders (e.g., primary, secondary, tertiary). By using this formalism in

a single operation, one can calculate the abundances at the sources given the observed fluxes of nuclei, or obtain the fluxes expected to be observed for any given source composition. This formalism is valid, including for radioactive nuclei, as long as appropriately averaged values of the density of the ISM and other parameters were adopted, as in the case of the LB model. At the Fourteenth International Cosmic Ray Conference, held in 1975 in Munich, Germany, the same authors (37) presented further details of their nested leaky-box (NLB) model and suggested that positrons at $E \gtrsim 10$ GeV should have nearly the same spectrum ($\sim E^{-2.7}$) as the protons at $E \gtrsim 100$ GeV that generated them.

At the same conference, Lachièze-Rey & Cesarsky (38) showed that in their EDL models the positron and antiproton spectra fall steeply at high energies. Accordingly, they suggested that future observations of positron and antiproton spectra in cosmic rays would provide good tests to distinguish between NLB and EDL models, and that antiprotons would provide the better test. Cesarsky (5) reiterated this last point in her article on models of cosmic-ray propagation. Thus, the precise observations of positrons and antiprotons that were recently made with the BESS, PAMELA, and AMS instruments are providing us with the requisite data to apply the test suggested by Cesarsky, which will enable us to answer a fundamental question in cosmic-ray physics that underlies the more general problem of the origins of cosmic rays. These and other recent observations are also having a broad impact on fields such as cosmology and particle physics.

1.2. A Quick Overview of Relevant Cosmic-Ray Observations

Since the publication of Cesarsky's 1980 review (5), there has been considerable progress in the field of cosmic rays, and new areas of interest have emerged, involving antiparticles in cosmic rays serving as probes of the nature of Galactic dark matter. Most importantly, the instruments used to observe cosmic rays have become progressively more sophisticated, and we now have very good spectra of the total electronic component, resolved into electrons and positrons (39) as well as protons and antiprotons (40–43). Before delving into these topics, I describe the most recent observations of cosmic rays relevant to this review. **Figure 1** displays the spectral ratio of positrons and antiprotons to protons; **Figure 2** presents the ratio of B to C nuclei as a function of energy; and **Figure 3** shows the bounds on the anisotropy of cosmic rays. Most of the discussion in this section is based on these observations. When looking at these ratios, one should keep in mind the generic interconnections among the various components.

1.3. A Perspective on Dark Matter

Knowledge of the existence of unseen gravitating matter dates to 1933, when Zwicky (3) measured the speeds of galaxies in the Coma Cluster, revealing an apparent violation of the virial theorem:

$$\Sigma m_i v_i^2 > \frac{1}{2} \sum \frac{G m_i m_j}{|\mathbf{r}_i - \mathbf{r}_j|}. \qquad 7.$$

Zwicky suggested that the presence of some unseen matter, which he named dark matter, should be present in the cluster to account for this virial discrepancy. Around the same time, Oort (53) studied the motions of stars, transverse to the Galactic plane and close to the solar neighborhood, and suggested that there could exist more matter than what was observed, contributing to the gravitational potential of the Galactic disc. Separate confirmations of the existence of such unseen matter came in the 1970s. First, Rubin & Ford (54) observed the rotation of the Andromeda Galaxy by following an early suggestion by Babcock (55); Bosma (56) posited that this rotation was due to an extensive halo of dark matter surrounding the galaxies. Second, Rood et al. (57)

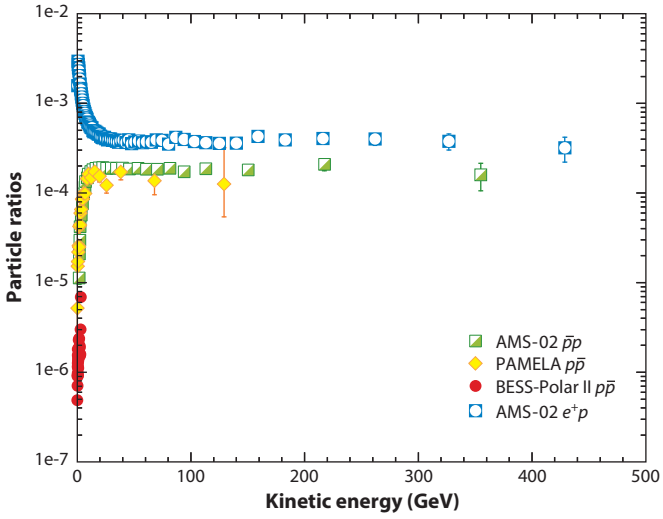

Figure 1

The ratios of the spectral intensities of positrons (39) and antiprotons (41–43) to that of protons (40) in cosmic rays. The near flatness of this ratio at high energies highlights their generic connection and suggests that the leakage lifetime of cosmic rays from the Galaxy is nearly independent of energy.

confirmed the virial discrepancy in the Coma Cluster of galaxies. Immediately thereafter, Cowsik & McClelland (58) suggested that this unseen matter was in fact made up of weakly interacting particle relics from the Big Bang and that these dominated the formation of large-scale structure in the dynamics of the Universe. These considerations also implied a bound on the masses of weakly interacting particles such as the neutrinos (59–61) of less than a few eV.

The crucial connection to much of the current interest in dark matter, including its possible contribution to the energetic positrons and antiprotons in cosmic rays, was made by Lee & Weinberg (62), who noted that the assumption by Cowsik & McClelland (58) that neutrinos do not annihilate in their evolution subsequent to decoupling is valid only for light neutrinos. By contrast, for hypothetical heavy neutrinos, annihilation plays a role in diminishing their cosmological number density, and weakly interacting particles with masses of several GeV could be contributing as much as the critical density of the Universe. Such particles that were nonrelativistic at the epoch of decoupling and that survive today with significant density are called weakly interacting massive particles (WIMPs), and they constitute the cold dark matter (CDM) in the Universe. Steigman et al. (63) have calculated the average density of WIMPs. Following accepted practice, we present all the cosmological densities as their ratios with respect to the critical density, ρ_c:

$$\rho_c = \frac{3H_o^2}{8\pi G_N} = 1.05 \times 10^{-5}\, h^2 \text{ GeV cm}^{-3}. \quad 8.$$

Here, the Hubble constant $H_o = 100\, h$ km s^{-1} Mpc^{-1}. For convenience, we take $h = 0.678$, obtained by fitting Planck data (64) to ΛCDM cosmology (65), in quoting other values. The mean dark matter density in the Universe, Ω_{DM}, in units of the critical density, is

$$\Omega_{DM} = 0.267, \quad 9.$$

which corresponds to $\rho_{DM} \approx 2.8 \times 10^{-6}$ GeV cm^{-3}. In order to yield this density, the rate of annihilation (63) for dark matter particles should be

$$\langle \sigma_A v \rangle \approx 2.1 \times 10^{-26} \text{ cm}^3 \text{ s}^{-1}. \quad 10.$$

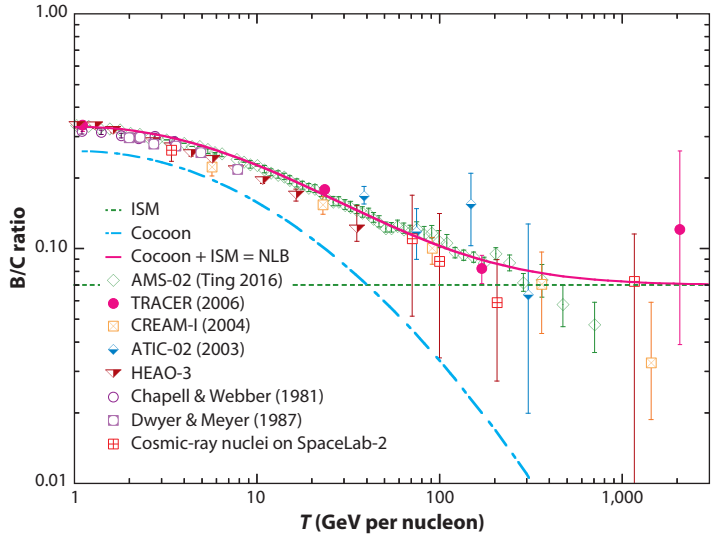

Figure 2

The observed B/C ratio (44–51, 113–115) along with the ratio expected in the nested leaky-box (NLB) model (113, 114). The solid line represents the prediction of the NLB model, whose parameters are determined by fitting exclusively to AMS data. The dash-dotted line represents the contribution of the cocoon, and the dotted line represents the contribution from spallations in the interstellar medium (ISM).

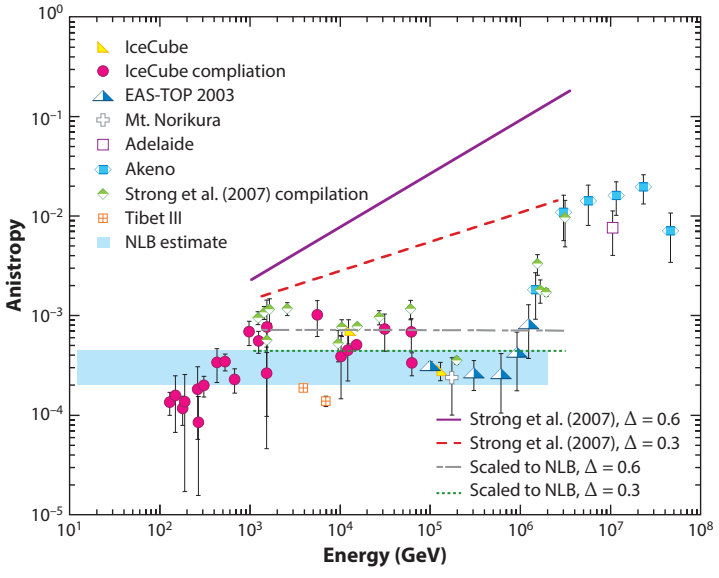

Figure 3

Measurements of the cosmic-ray anisotropy compiled by Cowsik & Burch (52). Also plotted are the predictions from energy-dependent leakage models by Strong et al. (10) and the scaled values for the nested leaky-box (NLB) model from Cowsik & Burch (52, equation 7). The light blue region shows the predicted anisotropy for the NLB model from Cowsik & Burch (52, equation 8).

Here enters the main theme of this discussion: the positrons and antiprotons in cosmic rays. The formation of galaxies, including our own, was triggered by the initial growth of density enhancements in dark matter. Subsequent to decoupling from radiation at a redshift of ∼1,100, normal matter fell into the gravitational potential wells generated by dark matter concentrations (see, e.g., Reference 65). Accordingly, the density of dark matter in galaxies, including our own Milky Way, is enhanced considerably with respect to the mean value ρ_{DM} in the Universe:

$$\rho_\chi \approx 0.3\,\mathrm{GeV\,cm^{-3}}. \qquad 11.$$

With such a high density of dark matter permeating and enveloping our Galaxy, there is a significant rate of annihilation and possibly decay; this process produces the familiar particles of the Standard Model, including positrons and antiprotons. Because these are charged and energetic particles, they diffuse in the Galactic volume and build up their density over millions of years, in a manner similar to cosmic rays, and constitute a background that can be searched for by direct and indirect detection experiments in order to probe the nature and mass of dark matter particles. As the Galaxy is made up of matter, we expect a negligible amount of antiparticles in the primary cosmic rays, and the only background to contend with is that generated by the interactions of primary cosmic rays. Accordingly, the energetic positrons and antiprotons constitute a highly accessible channel for the study of Galactic dark matter. Any positive identification of a signal would have a transformative impact on our understanding of several fields of study, ranging from cosmology and Galactic dynamics to cosmic rays and particle physics beyond the Standard Model.

1.4. Distribution of Dark Matter in the Galaxy

In order to estimate the contribution of the decay and annihilation of the particles constituting Galactic dark matter to the fluxes of positrons and antiprotons in cosmic rays, we need to know how dark matter is distributed across the Galaxy. There are basically two approaches to determining the distribution of dark matter in our Galaxy, and both have been extensively investigated.

1.4.1. Mass density models of the Galaxy. In determining the distribution of dark matter—especially in the context of its direct and indirect detection—the mass and luminosity distribution of various baryonic components of the Milky Way and the kinematics of their motion play important roles. Studies in this area were begun by Jeans (67) in 1922, followed by Oort (68) in 1932; Schmidt (69) developed a full-fledged model in 1956. Following the realization of the importance of dark matter for structure formation and Galactic dynamics, researchers began systematically developing mass models. This research culminated in work by Binney & Dehnen (70), who focused on the spheroidal nature of the Galactic halo and its ability to accommodate a variety of astronomical observations, including rotational velocities in the inner Galaxy, Oort constants, the local surface density of the disk (71, 72), and the satellites of the Milky Way. More recently, Weber & de Boer (73) and McMillan (74) used Bayesian and Markov chain Monte Carlo analyses to fix the parameters of the mass models. Improvements in the computational capacity to address structure formation in the Universe, leading up to the Millennium Simulation (75), have led to parameterized fits to the density distribution [e.g., fits by Navarro et al. (76) and others], which often showed a central cusp. Whether or not a cusp in the density distribution at the center of our Galaxy exists is not settled. In order to analyze the observations pertaining to the decay of dark matter particles, the following

set of parameters that is consistent with the rotation curve of the Galaxy has been chosen:

$$v_r(r) = \sqrt{|r\frac{\partial U}{\partial r}|}. \qquad 12.$$

Here, U is the total gravitational potential of the Galaxy, including the contributions of both baryonic and dark matter. Some of the frequently used forms of the density profiles for dark matter can be written in the generalized form

$$\rho_\chi(r) = \rho_0 \left(\frac{r_\odot}{r}\right)^\gamma \left\{\frac{1+(r_\odot/r_s)^\alpha}{1+(r/r_s)^\alpha}\right\}^{(\beta-\gamma)/\alpha}. \qquad 13.$$

In these density profiles, r is the galactocentric radius; ρ_0 is the density parameter; $r_\odot$ is the galactocentric distance of the Sun; and r_s, $\propto$, β, and γ are adjustable parameters.

1.4.2. Models based on phase-space distributions. These models assume an appropriate form of the distribution function $f(v, r)$ for particles of dark matter, such as lowered isothermal distribution (77). This distribution is characterized by two independent parameters, one related to the density of dark matter and the other related to its velocity dispersion; the distribution satisfies the stationary collisionless Boltzmann equation. One solves the Poisson equation to obtain the potential U_χ due to dark matter and, thus, the density distribution as a function of position:

$$\nabla^2 U_\chi = 4\pi G\rho_\chi, \qquad 14.$$

$$\rho_\chi(r) = \int f(v, r)d^3v. \qquad 15.$$

As the lowered isothermal distribution function f depends on the total potential $U_{\rm tot}$, which is the sum of U_χ due to dark matter and U_v due to visible matter, the Poisson equation is a self-consistent nonlinear coupled equation that is solved by numerical methods. This approach was initiated by Cowsik and his collaborators (see References 78 and 79 for details). Recently, Burch & Cowsik (80) presented an extensive compilation of the density distributions of all forms of baryonic matter in the Galaxy for use in deriving the potential $U_v(r)$ generated by visible matter. After solving for the potential $U_\chi(r)$ as a function of the two parameters characterizing $f_\chi(v, r)$, the authors made a detailed comparison between the consistency of the total potential and the observed kinematics, such as the rotation curve of the Galaxy and stellar velocity distributions, including those of the blue horizontal-branch stars situated at large distances in the dark matter halo of the Galaxy. **Figure 4** shows the density distribution $\rho_\chi(r)$ as a function of the galactocentric radius r, along with the Navarro–Frenk–White (NFW) profile (76), obtained by setting $\alpha = 1$, $\gamma = 1$, and $\beta = 3$ in Equation 13, which matches the theoretical curve surprisingly closely.

2. COSMIC-RAY MODELS WITH ENERGY-DEPENDENT LEAKAGE SPECTRA OF POSITRONS AND ANTIPROTONS

The observed decrease of the ratio of secondary nuclei (such as B) to the primary cosmic-ray nuclei that produce them (such as C and O), combined with the fact that spallation cross sections are independent of energy, naturally led to the suggestion that primary cosmic rays spend less time with increasing energy in the ISM, where all the spallation reactions were assumed to take place. This suggestion is the essence of the EDL models (24) and has been developed extensively over the years. A direct and almost inseparable consequence of this assumption of EDL of cosmic rays from the Galaxy is that the ratio of other secondary particles (such as positrons and antiprotons) to their

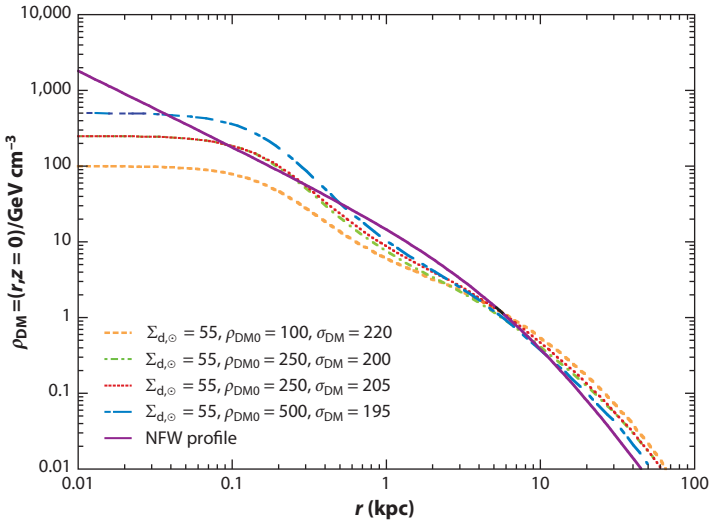

Figure 4

The theoretical estimate of the density profile of dark matter in the Galaxy, derived self-consistently from considerations of phase space by Burch & Cowsik (80). Here, Σ refers to the column density of the Galactic disk at the solar circle (in units of Mpc^{-2}), ρ_{DM0} is the density of dark matter at the center of the Galaxy (in units of GeV cm^{-3}), and σ is the dispersion parameter but not the dispersion in the velocities of dark matter particles. These profiles are also consistent with all the measured motions of stars and gas in our Galaxy. The solid purple line represents the Navarro–Frenk–White (NFW) profile (76) based on a fit to numerical simulations of galaxy formation.

progenitors (such as protons) also falls with energy, contrary to recent observations (**Figure 1**). Accordingly, the discussion of these models is brief, and I focus on suggestions for ways to make them conform to the observations.

As mentioned above, the EDL model for cosmic-ray propagation proposed by Audouze & Cesarsky (24) stimulated considerable interest, prompting the development of the GALPROP code and its application to interpret the spectra of protons and electrons produced by cosmic rays (81). The GALPROP code incorporates in detail a variety of astronomical observations of the Galaxy, making it a powerful tool for the study of cosmic-ray propagation and the spectra of various secondary components, including secondary nuclei, antiprotons, and positrons. The GALPROP code has also been very useful in providing a good description of the diffuse γ-rays arising from π^0 decay, bremsstrahlung, and inverse Compton scattering in the Galaxy. An alternate code, DRAGON, has been written (82) and semianalytical methods have been used to solve the propagation equations (19), both in the context of EDL. I refer to these models collectively as the EDL model.

On the basis of theoretical inputs from Parker (83, 84), Gleeson & Axford (85), and many others [as elegantly summarized by Berezinskii et al. (20)], the following general transport equation is solved under the assumption of steady-state conditions:

$$\frac{\partial \psi(\vec{r}, p, t)}{\partial t} - \nabla \cdot (D_{r,r} \nabla \psi - \mathbf{V}_c \psi) - \frac{\partial}{\partial p} p^2 D_{pp} \frac{1}{p^2} \psi + \frac{\partial}{\partial p} \left[\dot{p} \psi - \frac{p}{3} (\nabla \cdot \mathbf{V}_c) \psi \right] + \frac{1}{\tau_f} \psi + \frac{1}{\tau_r} \psi = q(\vec{r}, p, t). \quad 16.$$

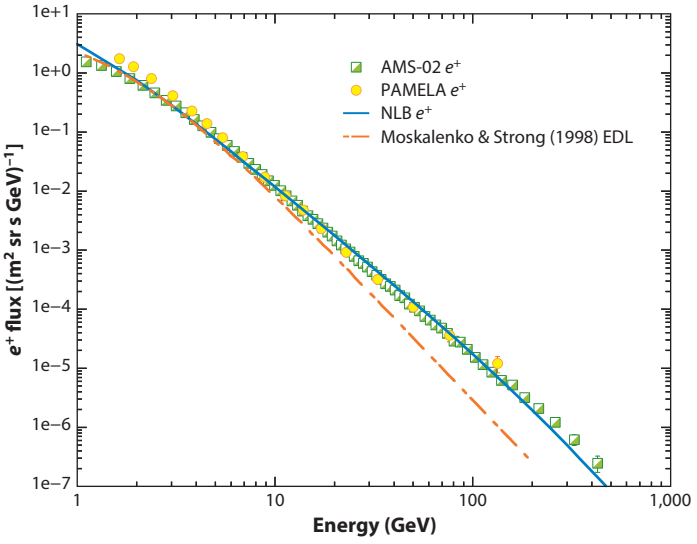

Figure 5

The predictions of the spectrum of positrons in cosmic rays by the energy-dependent leakage (EDL) model (10) and the nested leaky-box (NLB) model (112), compared with observations (39, 154). The increasing leakage loss predicted by the EDL model leads to steeper spectral intensities, below the observations at high energies. The NLB model fits the observations well up to ∼200 GeV, beyond which the theoretical spectrum steepens due to radiative energy losses.

Here, $\psi(r, p, t)$ is the density of particles at momentum p, and $q(r, p, t)$ is the source function that is usually solved under steady-state conditions by taking into account diffusion and convection in r and p, losses due to spallation in collisions with interstellar gas included as a time constant τ_f, and radioactive decay with a time constant τ_r. This versatile equation, containing many parameters allowing the spatial and momentum dependence of the transport parameters and the source functions to be specified, is solved in a cylindrical volume whose dimensions can be specified as desired, and the condition that $\psi(\vec{r}, p, t)$ vanishes at the boundary is imposed. The momentum dependence $D_{rr} \sim D_0\rho^\delta$ for rigidities $\rho > \rho_0$, and possibly a different dependence below ρ_0, along with appropriate choices of all other parameters, is chosen to fit the observed B/C ratio, thereby defining the model. This model has been discussed extensively in the literature (10, 19, 81, 86–98), so I limit this discussion to examples of the predictions of the spectra of positrons and antiprotons in the EDL model (**Figures 5** and **6**). Note that both of these spectra are significantly steeper than the observed spectra; this is a generic feature of the EDL model and, indeed, of any model assuming that spallation products such as B nuclei are generated exclusively in the ISM, where most of the positrons and antiprotons are produced by high-energy interactions of cosmic rays.

A consensus view of the best values for these parameters has not yet emerged. However, the EDL model has provided a good fit to the observed spectra of the primary nuclear and total electronic components to the B/C ratio, as well as good estimates of the diffuse γ-ray emission observed from the Galaxy. A weakness of the model, as pointed out by Strong et al. (10), is that it predicts large anisotropies violating observational bounds (**Figure 3**). In other words, the mean free path λ for the scattering of cosmic rays in the ISM is given by $\lambda = 3D_0(\rho/\rho_0)/c^\delta \approx$ 4 kpc at 5×10^5 GV for $D_0 \approx 2 \times 10^{28}$ cm^{-2} at $\rho_0 = 4$ GV and $\delta = 0.75$ (92). With such a large mean free path, the cosmic rays arrive at the Earth with high probability without having suffered any scattering at all from the sources that lie at distances $d \lesssim \lambda$. Such scattering-free

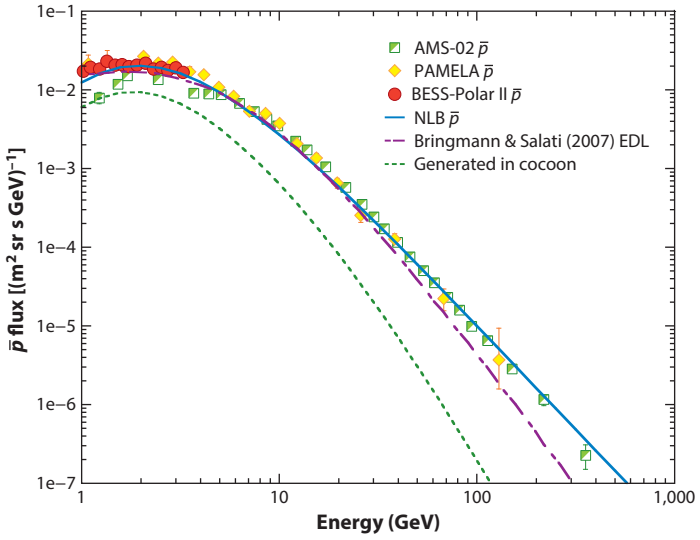

Figure 6

The observed spectral intensities of the antiprotons in cosmic rays (41–43), compared with the predictions of the energy-dependent leakage (EDL) model (111) and the nested leaky-box (NLB) model (114). The predicted EDL spectrum is steeper than that observed. The NLB model provides a good fit, indicating that τ_G is constant, independent of energy. Because the antiprotons do not suffer radiative loss of energy during their transport, they provide a better test of the constancy of τ_G at these energies. The dashed green line represents the contribution of the cocoons to the antiproton intensities (113, 114).

propagation causes the cosmic-ray intensity to display narrow peaks in the directions of such sources, contrary to observations. The predictions related to positrons and antiprotons resulting from these models are taken as the background for assessing contributions from sources other than cosmic-ray interactions, such as annihilation or decay of dark matter, or emission from astrophysical sources, such as pulsars and supernova remnants.

The finding that even early observations of positrons and antiprotons clearly disagreed with the well-developed EDL model stimulated investigations of alternate sources (88–98), such as nearby pulsars or million-year-old supernova remnants, or additional effects during acceleration of cosmic rays in supernova shocks. The basic explanation for this discrepancy (88, 90, 92, 93) rests on an early result showing that when secondary particles are produced by primary cosmic rays during their acceleration process, the ratio of secondary to primary particles increases monotonically with energy (99, 100). It was suggested that such acceleration of secondary positrons and antiprotons took place in supernova shocks, and the expected increase might compensate for the more rapid leakage from the Galaxy in EDL models at high energies and thereby reproduce the observations. The mechanism inducing this increase in the secondary-to-primary ratio would, of course, operate equally well with other ratios, such as B/C, contrary to observations (101). To overcome these objections, Mertsch & Sarkar (92) introduced a cutoff at $E_{\max}$ up to which such acceleration of secondary particles may proceed in supernova remnants, even though the acceleration of primary particles is expected to go on or up to much higher energies. These authors showed that, although adequately good fits to the $e^+/(e^+ + e^-)$ and B/C ratios are possible, the predictions for the ratio of antiprotons to protons tend to exceed the observed ratios even for the lowest choice of the parameter, $E_{\max} = 1{,}000$ GeV.

The other idea for obtaining the current positron fraction is that the primary sources of electrons are inhomogeneously distributed (102–104), for example, with a concentration of supernova

remnants toward the spiral arms in contrast to the secondary positrons generated in the ISM. Cowsik & Lee (105) and Nishimura et al. (106) investigated the effect of such finite distances of the sources, as did Cowsik & Burch (52) in the context of the positron fraction in the NLB model. Several possible ways to generate the missing flux include leakage of the relativistic electron–positron plasma from pulsar magentospheres, local inhomogeneities in the Galactic structure, and an ancient supernova in the solar neighborhood. For a review of some of these suggestions and additional references, see Israel (107); see Yuan et al. (104) for an analysis showing that it is generally difficult to fit simultaneously the total spectrum of the electronic component and the positron fraction with the same set of parameters in these alternate source models. Critical assessments by Katz et al. (108) and Blum et al. (109) suggest that positrons could be simply cosmic-ray secondaries and that no new sources are needed. This idea is also endorsed by Kruskal et al. (110).

3. NESTED LEAKY-BOX MODEL: CURRENT PERSPECTIVE

The NLB model fits the observed B/C ratio and the spectral intensities of the positrons and antiprotons without invoking dark matter or any other new sources (52, 112–114). The essential physics exploited in the NLB model is that B nuclei produced in spallation reactions emerge with the same energy per nucleon as their parents, such as C and O; by contrast, positrons and antiprotons are produced in interactions of protons of much higher energies. We now have excellent measurements of the Li/C and B/C ratios extending to energies beyond ~100 GeV per nucleon, as well as bounds on cosmic-ray anisotropies. These observations complement the information obtained from the spectral intensities of the electronic component, positrons and antiprotons. Before discussing how the differences in the kinematics of the production of secondary nuclei such as B, positrons, and antiprotons allow a consistent interpretation of the decreasing B/C ratio, together with the nearly flat positron-to-proton and antiproton-to-proton ratios, we describe and comment on the basic assumptions of the NLB model:

1. Cosmic-ray sources are born across the Galactic disc, randomly in space and time once in T_b years, and function as sources for a period of $\sim T_d$ years. Thus, at any time an average of $N_s = T_d/T_b$ sources are active in the disc. If Galactic cosmic rays fill a volume V_G, then the number density of these sources is $n_s = N_s/V_G$. For example, supernova remnants with $T_b \sim 50$ years and $T_d \sim 10^5$ years yield $N_s \approx 2{,}000$ across the entire Galaxy. Therefore, the effects of the temporal discreteness of the sources are not particularly important here.
2. The sources accelerate primary cosmic rays with spectra very similar to those observed at $\sim E^{-2.7}$ at energies above ~10 GeV per nucleon. Suppose each of the sources generates primary cosmic rays at a rate $s_i(E)$ of the form

$$s_i(E) = s_{i,o} E^{-p}. \tag{17.}$$

These nuclei come out without much loss, and contribute an average source term

$$q_i(E) = n_s s_{i,o} E^{-p}\ \mathrm{cm}^{-3}\mathrm{s}^{-1}\mathrm{GeV}^{-1}. \tag{18.}$$

If τ_G is the leakage lifetime of cosmic rays from the Galaxy, then there is a flux of primary cosmic rays, given by

$$F(E) = \frac{\beta c \tau_G}{4\pi} q_i, (E) = \frac{\beta c \tau_G}{4\pi} n_s s_{i,o} E^{-p} \mathrm{cm}^{-2}\mathrm{s}^{-1}\mathrm{sr}^{-1}\mathrm{GeV}^{-1}. \tag{19.}$$

In order to match the observations, the spectral index p in the source term $q_i(E)$ must be chosen to be 2.7 or 2.6 at high energies, the same as that observed in the interstellar space. For all the results quoted here, p is taken to have a nominal value of 2.7. Note that this choice of the spectral index differs from the requirement of the EDL model, which requires

p to be in the range from 2 to 2.4 to compensate for the more rapid leakage of particles at higher energies. To connect these different requirements of the two models with the theories of cosmic-ray origins, we note that the acceleration of cosmic rays in plane parallel shocks (25–28) yields $p = (x + 2)/(x - 1)$, where x is the compression ratio. For a high–Mach number shock, $x = 4$, which yields $p = 2$. By contrast, recent research (116–119) has shown that the value of x could be smaller. For example, Blasi et al. (116) have suggested that neutral atoms present in the shocks can transfer the mass and momentum across the shock to lower the compression ratio; for $x \approx 2.8$, spectra with the requisite spectral indices in NLB models could be generated.

3. The cosmic-ray sources are surrounded by a clumpy shell of stellar debris, termed the cocoon, as indicated by several observations and theoretical considerations (120–123). The residence time of cosmic rays in this region is a decreasing function of energy (112–114),

$$\tau_c(E) = \tau_0 T^{-\zeta \ln T}, \qquad 20.$$

where $\zeta \approx 0.1$ for T (in GeV per nucleon). This energy-dependent transport was chosen to fit the energy-dependent part of the B/C ratio (**Figure 2**) and is similar to the increase in the diffusion constant of cosmic rays in the solar wind (124). The functional form is also supported by the γ-ray spectra observed from several Galactic sources (125).

4. Once cosmic rays leak from the cocoon, they diffuse in the general ISM and leak out of the Galaxy into the intergalactic medium. This transport is taken to be independent of the cosmic-ray energy up to almost 10^6 GeV, and is characterized by a lifetime, τ_G, given by

$$\tau_G \approx 2.3\text{My}. \qquad 21.$$

This energy-independent lifetime, implying constancy of the diffusion constant, is consistent with observations of the density inhomogeneities in the ISM. An extensive review and analysis by Armstrong et al. (126) provides information about spectral densities over a wide range of wave numbers k. For a typical magnetic field strength of $\sim$5 μG, the wave numbers that are relevant for cosmic-ray transport in the energy range from a few GeV to a few TeV are in the band $10^{-10}\ \text{m}^{-1} < k < 10^{-13}\ \text{m}^{-1}$. In this band, the observed spectral densities fit very well with

$$F(k)d^3k \sim k^{-\xi} d^3k \sim k^{-4} d^3k. \qquad 22.$$

Accordingly, the dependence of the diffusion constant (3) on rigidity ρ is given by

$$D(\rho) \sim \beta \rho^{4-\xi} \sim \beta \rho^0 \sim \text{constant}. \qquad 23.$$

Lewandowski et al.'s (127) observations of the variation of pulsars' pulse width with frequency also support the k^{-4} form of the spectral intensities.

In the following section, I compare the fluxes and flux ratios expected in the NLB model with those from observations. I begin with the B/C ratio, which is used to determine the parameters of the model.

3.1. The B/C Ratio in Cosmic Rays

The kinematics of the production of B nuclei through the spallation of heavier nuclei is very simple: B emerges with very nearly the same kinetic energy per nucleon as its parent nuclei. Furthermore, at energies above a few GeV per nucleon, the spallation cross sections are independent of energy, and the energy loss due to ionization can be neglected. Consequently, the B/C ratio is proportional

to the sum of the grammages λ traversed in the cocoon and in the ISM:

$$\mathrm{B/C} \propto \beta c m_{\mathrm{H}} (n_{\mathrm{H,c}} \tau_{\mathrm{c}}(E) + n_{\mathrm{H,ISM}} \tau_G) \sim (\lambda_{\mathrm{c}} + \lambda_G). \quad 24.$$

Here, $n_{\mathrm{H,c}}$ and $n_{\mathrm{H,ISM}}$ are the mean number densities of H atoms (which act as targets for spallation) in the cocoon and in the ISM. **Figure 2** compares this form of the B/C ratio expected in the NLB model with observations. The fit is very good up to ~250 GeV per nucleon, and reproduces the dependence of the ratio on energy, including the tendency of the ratio to level off beyond ~60 GeV per nucleon. At ~300 GeV per nucleon and above, there are five data points with larger uncertainties that do not show any clear trend. Data acquired with improved statistics and smaller systematic uncertainties will more accurately fix the value of τ_G postulated in the NLB model. These data should become available in the next few years from the AMS and CALET instruments (128), as well as from ISS-CREAM (129), which will also be located on the International Space Station. The charge resolution of AMS (1) ensures that Li fluxes are free from contamination by neighboring elements. Accordingly, the observed spectrum of Li nuclei (1) with an index of −2.7 at high energies lends strong support to the NLB model with τ_G constant. As both Li and B are spallation products of C and heavier elements, the NLB model predicts similar energy dependences for Li/C and B/C ratios.

3.2. Cutoff in the Spectrum of Electrons

In the NLB model, the discrete nature of the sources implies that particles emitted from those sources will take a finite amount of time to diffuse up to the Earth, depending on their distance. This finite time interval between production and observation induces a cutoff in the spectrum of electrons, of the form $\sim \exp\left(-r_i^2 b E/4D\right)$, where r_i is the distance to the source, $\left(-bE^2\right)$ is the rate of radiative energy loss in the Galaxy, and D is the diffusion constant, taken to be independent of energy in the NLB model. For typical numbers, the loss of energy through the emission of radiation leads to a cutoff at ~1 TeV in the spectrum of electrons arriving from even the nearest source at $r_n \approx 400$ pc, as shown by Cowsik & Lee (105), Nishimura et al. (106), and more recently Cowsik et al. (52, 112) in the context of the $e^+/(e^+ + e^-)$ ratio. The relevance of such effects on the positron fraction in the EDL model is noted in Section 2, above.

3.3. The Positron Spectrum and the Positron Fraction

Positrons are generated by high-energy interactions of cosmic rays producing energetic π^+, which yield positrons through the decay chain $\pi^+ \rightarrow \mu^+ + \nu_\mu$, $\mu^+ \rightarrow e^+ + \nu_e + \bar{\nu_\mu}$. The rate of positron generation has been calculated by several authors; we adopt the calculation by Moskalenko & Strong (81). An essential kinematical feature of the production process is that positrons typically carry away only ~5% of the energy of the primary protons. As a consequence, the energy of the primary particles needed to generate positrons above 10 GeV is in excess of ~200 GeV per nucleon. At such high energies, as shown by Equation 20, the cosmic rays rapidly diffuse across the cocoon without producing a significant number of positrons. Given that we are interested in higher energies, we may neglect the production of positrons in the cocoon and focus on their production in the ISM. Negatively charged electrons are also produced by the interactions of cosmic rays, but because protons dominate over neutrons in the cosmic-ray flux, the flux of electrons generated is approximately one-half that of positrons, when we take into account multiplicity in pion production.

The source function for the positrons in the ISM is given by

$$q_{e^+}(E) = q_+ E^{-p}, \quad 25.$$

where $q_+ \approx 5 \times 10^{-27}$ cm^{-3} s^{-1} GeV^{-1} (H atom)$^{-1}$ when E is expressed in GeV, and the spectral index $p \approx 2.7$ is equal to that of the protons in primary cosmic rays. If we assume that the ISM, on average, is nearly uniform and surrounds the Solar System, it is easy to show (17) that the positron flux in cosmic rays is given by

$$\begin{aligned} F_{e^+}(E) &= \int_0^{1/bE} \frac{c}{4\pi} n_{\mathrm{H,ISM}} \frac{q_+}{E^p} (1 - bEt)^{p-2} e^{-t/\tau_G} dt, \\ &= \frac{c}{4\pi} \tau_G n_{\mathrm{H,ISM}} \frac{q_+}{E^p} \quad \text{for} \quad E << 1/b\tau_G, \\ &= \frac{c\,\tau_G n_{\mathrm{H,ISM}}}{4\pi b\,(p-1)} \frac{q_+}{E^{p+1}} \quad \text{for} \quad E >> 1/b\tau_G. \end{aligned} \tag{26.}$$

For the choice $n_{\mathrm{H}} = 0.5$ cm^{-3} (H atom)$^{-1}$ and $\tau_G = 2.3$ My, we have performed a numerical integration of Equation 33, below, and applied a small correction to account for the solar modulation effects at low energies in order to obtain the positron spectrum expected in the NLB model. The fit to the observations shown in **Figure 5** is good up to ~150 GeV; beyond this value, the theoretical curves show a gentle transition toward a steeper spectrum and have an asymptotic form $E^{-3.7}$.

Because the positron spectrum is reproduced faithfully in the NLB model, the increase in the positron fraction can be understood in terms of the spectra of primary electrons accelerated in the sources and observed with a spectral slope of ~3.2 beyond 10 GeV and a sharp steepening beyond ~1 TeV, leading to a cutoff in the spectrum. At these high energies, the secondary positrons and electrons generated in the nearby regions of the ISM will have a spectral index of ~3.7 and will dominate the observed intensities. Because these are secondary cosmic rays, they are generated with a positron fraction of ~0.66, and accordingly, we expect the observed intensities to reach this value at energies well beyond a few TeV.

3.4. Cosmic-Ray Antiprotons in the Nested Leaky-Box Model

The observed antiproton-to-proton ratio is independent of energy beyond ~10 GeV (**Figure 1**). This similarity in their spectra implies a generic connection between the protons and antiprotons and indicates that the residence time of cosmic rays is essentially constant, independent of energy. The kinematics of the production of antiprotons by energetic protons is interesting for several reasons: The threshold energy of the primary particle is $7m_p \approx 6.5$ GeV, and the antiproton emerges from the interaction with a kinetic energy of $m_p \sim 0.94$ GeV. As the energy of the primary particle increases, the spectrum of the emerging antiproton spreads toward both lower and higher energies. As a consequence of the increase in multiplicity and the power-law spectrum of cosmic rays, the observed spectrum has a peak just above the threshold, at ~2 GeV.

Many researchers have presented the cross sections for the production of antiprotons by cosmic rays in terms of analytical fits to the Lorentz-invariant product $G = E\frac{d^3\sigma}{dp^3}$ obtained from accelerator experiments (87, 130–135). Two aspects of these analytical fits are distinctive for cosmic rays: The decay of antineutrons and antihyperons has to be added in, and the contributions of nuclei such as helium must be accounted for, both in the primary beam and in the target (132, 133). Given the parameterized form of G, the differential cross section for the production of an antiproton of energy E by a primary proton with energy E_p colliding with a target proton is

$$\begin{aligned} \frac{d\sigma(E, E_p)}{dE} &= \int_0^{\theta_x} \int_0^{2\pi} \frac{G}{E} p^2 \frac{dp}{dE} \cdot \sin\theta d\theta d\varphi, \\ &= \int_0^{\theta_x} 2\pi G\, p_{\mathrm{T}}\, d\theta, \end{aligned} \tag{27.}$$

where $p = \sqrt{E^2 - m_p^2}$; $\frac{dE}{dp} = \frac{E}{p}$; and $p_T = p\sin\theta$, the transverse momentum of the antiprotons. The upper limit θ_x arises from kinematics and is given by

$$\theta_x = \cos^{-1}\left[\frac{(E_p + m_p)(E - m_p) + 4m_p^2}{(E_p + m_p)^{1/2}(E_p - m_p)^{1/2} \cdot p}\right]. \quad 28.$$

In the NLB model there are two source terms. The first is due to production in the cocoons $q_{\bar{p},c}(E)$, and the second is due to production in the ISM, $q_{\bar{p},ISM}(E)$:

$$q_{\bar{p},c}(E) = n_s \int_{E_{th}(E)}^{\infty} s_p(E_p) c\tau_c(E_p) n_{H,c} \frac{d\sigma(E_p, E)}{dE} \cdot dE_p,$$
$$= \int_{E_{th}(E)}^{\infty} q_p(E_p) \tau_c(E_p) n_{H,c} \frac{d\sigma(E_p, E)}{dE} \cdot dE_p. \quad 29.$$

Here, n_s is the mean number density of sources in the Galactic disc; $s_p(E_p)$ is the injection rate of protons per source; $q_p(E_p)$ is the mean injection rate per unit volume of the Galactic volume (as defined in Equations 17 and 18, above); and $\tau_c(E_p)$ is the EDL lifetime from the cocoon, leading to the grammage $\lambda_c = c\tau_c n_{H,c} m_H$, which is obtained by fitting the observed B/C ratio. The threshold energy $E_{th}(E)$ is obtained by solving for E_p after setting $\theta_x = 0$ in Equation 28. This source function for antiprotons, contributed by the interactions in the sources, yields an antiproton flux $F_{\bar{p},c}(E)$ in the ISM:

$$F_{\bar{p},c}(E) = \frac{c}{4\pi} q_{\bar{p},c}(E) \cdot X(E) \cdot \tau_G \text{cm}^{-2}\text{s}^{-1}\text{sr}^{-1}\text{GeV}^{-1}. \quad 30.$$

Here, $X(E)$ is an energy-dependent factor representing the contribution of He and other nuclei, both in the primary cosmic rays and in the target material (132, 136). This contribution (**Figure 6**) is significant in the energy range 1–5 GeV but is not as large as the contribution of cocoons to the B/C ratio because of the high threshold for antiproton production and the rapid decrease of the grammage in the cocoon at higher energies, as $\tau_c(E)$. Similarly, the contribution of cosmic-ray interactions in the ISM generates a flux of antiprotons that may be calculated as follows (**Figure 6**):

$$q_{\bar{p},ISM}(E) = \int_{E_{th}(E)}^{\infty} q_p(E_p) c\tau_G n_{H,ISM} \frac{d\sigma(E_p, E)}{dE} \cdot dE_P, \quad 31.$$

$$F_{\bar{p},ISM}(E) = \frac{c}{4\pi} q_{\bar{p},ISM}(E) \cdot X(E) \cdot \tau_G. \quad 32.$$

Note that this contribution dominates the spectrum at high energies. The sum of the two contributions $F_{\bar{p}}(E)$ fits the observed antiproton spectrum well at high energies but falls short of the flux observed below ~1 GeV. This very low energy component is attributed to the scattering of low-energy antiprotons and to the effects of adiabatic deceleration in the solar wind.

4. POSITRONS AND ANTIPROTONS IN COSMIC RAYS AS PROBES OF THE NATURE OF DARK MATTER PARTICLES

Even though there is no compelling need for a contribution from the decay or annihilation of dark matter in the NLB model, from the perspective of Galactic dynamics, particle physics, or cosmology, one cannot overestimate the importance of understanding the interaction, decay, and annihilation of these particles. The interconnection between the annihilation rate $\langle\sigma v\rangle$, which is close to the weak-interaction strength, and the density of dark matter, established in 1977 by Lee & Weinberg (62), stimulated astrophysical discussions aiming to identify the consequences of such

annihilation and searches for observable signals arising from them. Two of the earliest suggestions were to search for energetic antiprotons (137) and to search for γ-rays from astronomical systems (138). The same strategies and techniques suggested for the study of annihilation also apply to the study of decaying WIMPs, and these studies clearly complement efforts to directly detect scattering of Galactic dark matter particles off nuclei in the laboratory. Other reviews have summarized these wide-ranging efforts (139–142). The annihilation and decay are assumed to occur through W^+W^-, $Z\bar{Z}$, $b\bar{b}$, and other channels, and the positron, antiproton, γ-ray, and neutrino spectra emerging from these processes have been calculated with a state-of-the-art understanding of particle physics (143).

Currently, the best available limits of $\langle \sigma v \rangle$ arise from *Fermi*-LAT's (144) γ-ray observations of dwarf spheroidal galaxies associated with our Galaxy and fall below 2×10^{-26} cm^{-3} s^{-1} for this channel for $m_\chi \lesssim 100$ GeV. Observations from HESS provide the best bounds in the TeV domain of $\sim 10^{-25}$ cm^{-3} s^{-1} (145). Here, I focus on the antiparticles in cosmic rays, positrons and antiprotons, which may be stored in the Galactic volume for millions of years, enhancing the chance of their detection. Studies using the charged decay products, positrons and antiprotons, complement those using the neutral decay products, neutrinos and γ-rays. Each of these channels has its own advantages and uncertainties.

The search for positrons and antiprotons in cosmic rays arising from the decay and annihilation of dark matter has the advantage of the buildup of their intensities over millions of years. To interpret the observations of antiprotons and positrons, we need to calculate the contributions from the dark matter halo at the Earth that is situated close to the Galactic plane. Herein lies the difficulty: The halo of dark matter enveloping the Galaxy extends up to ~100 kpc or more. By contrast, all our knowledge about propagation of energetic particles in the Galaxy comes from observations of cosmic rays generated by sources close to the Galactic plane. It is in no way certain that the propagation parameters that are applicable close to the plane will hold true over such extended distances, where the strength and power spectrum of fluctuations of the magnetic field are expected to be quite different. There are two other reasons contributing to the difficulty of precisely estimating the fluxes of annihilation products of dark matter. The first involves the so-called boost factor, B, which represents the possible effects of local concentrations in the density of dark matter within the overall profile of the cloud of dark matter surrounding the Galaxy:

$$B_\chi = \langle \rho_\chi^2(r) \rangle / \langle \rho_\chi(r) \rangle^2 . \qquad 33.$$

The boost factor can, in principle, enhance the source function by a large factor (146). The second reason involves the Sommerfeld enhancement, which represents the increased rate of annihilation due to the possible existence of long-range attractive interactions on the annihilation of nonrelativistic particles (147).

Several groups have attempted to derive bounds on the decay lifetime and annihilation parameters of WIMPs in the EDL models (148–152). Here, I briefly summarize the findings of Hamaguchi et al. (153). These authors interpreted recent measurements of AMS-02 experiments on antiprotons as arising from decaying or annihilating dark matter with mass ~1 TeV or higher, in the context of an EDL model with propagation in a volume of radius ~20 kpc, a total halo thickness of 8 or 30 kpc, and a diffusion constant increasing with momentum as p^δ, with $\delta \approx 0.7$ or 0.46. The estimated annihilation cross sections $\langle \sigma v \rangle$ needed to fit the antiproton spectrum in the EDL model are $\sim 2 \times 10^{-24}$ cm^{-3} s^{-1} and 6×10^{-25} cm^{-3} s^{-1}, or decay lifetimes of 5×10^{26} s and 2×10^{27} s, respectively. The observed positron fluxes do not conflict with this interpretation. However, the annihilation cross sections needed are larger than $\langle \sigma v \rangle \approx 2.1 \times 10^{-26}$ cm^{-3} s^{-1}, required for the interpretation of dark matter particles as thermal relics in the standard ΛCDM cosmology (63). Perhaps the higher rate is attributable to the Sommerfeld enhancement or boost

effects. However, the cross sections are consistent with the upper bounds placed by *Fermi*-LAT's observations of dwarf spheroidal galaxies for $m_\chi \gtrsim 1$ TeV. The high value of $\delta \approx 0.7$ or $\delta \approx 0.46$ used in these models poses a concern because it implies a high level of anisotropy in cosmic rays, as does the large number of parameters that are assigned widely varying values by different analyses of the EDL models. Similar studies within the context of the NLB model have not yet been performed but would be useful.

5. EPILOGUE

During the last decade, a major effort has been launched to measure with high precision various cosmic-ray spectra, including those of antiprotons and positrons. The NLB model proposed by Cowsik & Wilson (32, 37) fits these observations in a simple and straightforward way. By contrast, the EDL model proposed by Audouze & Cesarsky (24) predicts positron and antiproton spectra that are steeper than the observations. Over the last few decades, researchers have devoted considerable effort to making the EDL model more sophisticated by including rigidity-dependent diffusion, convection, adiabatic deceleration, and stochastic acceleration in a multizone model for the Galaxy, along with spatially dependent source distributions. To date, there is no consensus on the values of the large set of parameters of the model, and the predicted positron and antiproton spectra are generally steeper than the observations. As a result, there have been extensive efforts to assess the contributions from new astrophysical sources, such as pulsars and old and nearby supernova remnants, and contributions from the decay and annihilation of Galactic dark matter particles. The estimated values of the lifetime and annihilation cross sections derived in these studies should be tentatively treated as bounds, in the absence of a consensus on models of cosmic-ray propagation and because the propagation parameters have been derived for sources concentrated in the Galactic plane, whereas the distribution of dark matter that permeates the Galaxy extends to ~100 kpc, with nearly equal source strength in each shell up to such distances. The NLB model provides a good explanation of the spectral intensities of positrons and antiprotons entirely as cosmic-ray secondary particles; nevertheless, because of the uncertainties in the cosmic-ray fluxes and interaction cross sections, there is still room for the discovery of new astrophysical phenomena and for an investigation of the properties of dark matter. The experimental and theoretical efforts needed to make these discoveries are the great challenge facing cosmic-ray scientists today.

DISCLOSURE STATEMENT

The author is not aware of any affiliations, memberships, funding, or financial holdings that might be perceived as affecting the objectivity of this review.

ACKNOWLEDGMENTS

I gratefully acknowledge extensive discussions with M.H. Israel, W.R. Binns, M.A. Lee, H. Volk, T. Gaisser, and P. Blasi. I thank T. Stumbaugh for help with preparation of the manuscript.

LITERATURE CITED

1. Ting SCC. *Proc. Sci.* ICRC2015:036 (2015)
2. Hess VF. *Phys. Z.* 13:1084 (1912)
3. Zwicky F. *Helv. Phys. Acta* 6:110 (1933)
4. Shapiro MM, Silberberg R. *Annu. Rev. Nucl. Part. Sci.* 20:323 (1970)

5. Cesarsky C. *Annu. Rev. Astron. Astrophys.* 18:289 (1980)
6. Trimble V. *Annu. Rev. Astron. Astrophys.* 25:425 (1987)
7. Wdowczyk J, Wolfendale AW. *Annu. Rev. Nucl. Part. Sci.* 39:43 (1989)
8. Gaitskell RJ. *Annu. Rev. Nucl. Part. Sci.* 54:315 (2004)
9. Feng JL. *Annu. Rev. Astron. Astrophys.* 48:495 (2010)
10. Strong AW, Moskalenko IV, Ptuskin VS. *Annu. Rev. Nucl. Part. Sci.* 57:285 (2007)
11. Anchordoqui LA, Montaruli T. *Annu. Rev. Nucl. Part. Sci.* 60:129 (2010)
12. Gaisser T, Halzen F. *Annu. Rev. Nucl. Part. Sci.* 64:101 (2014)
13. Ginzburg VL, Syrovatskii SI. *The Origin of Cosmic Rays.* New York: Pergamon (1964)
14. Hayakawa S. *Cosmic Ray Physics: Nuclear and Astro-Physical Aspects*. New York: Wiley Intersci. (1969)
15. Cowsik R, Pal Y, Tandon S, Verma RP. *Phys. Rev.* 158:1238 (1967)
16. Cowsik R, Pal Y, Tandon S, Verma RP. *Can. J. Phys.* 46:S646 (1968)
17. Cowsik R, Pal Y, Tandon S, Verma RP. *Phys. Rev. Lett.* 17:1298 (1966)
18. Jones FC. *Phys. Rev. D* 2:2787 (1970)
19. Maurin D, Donato F, Taillet R, Salati P. *Astrophys. J.* 555:585 (2001)
20. Berezinskii VS, Bulanov SV, Dogiel VA, Ptuskin VS. *Astrophysics of Cosmic Rays.* Amsterdam: North-Holland (1990)
21. Juliusson E, Meyer P, Müller D. *Phys. Rev. Lett.* 29:445 (1972)
22. Webber WR, Lezniak JA, Kish JC, Damle SV. *Nat. Phys. Sci.* 241:96 (1973)
23. Garcia-Munoz M, et al. *Astrophys. J.* 197:489 (1975)
24. Audouze J, Cesarsky CJ. *Nat. Phys. Sci.* 241:98 (1973)
25. Axford WI, Leer E, Skadron G. In *Proceedings of the 15th International Cosmic Ray Conference*, 11:132. Plovdiv, Bulg.: Bulg. Acad. Sci. (1977)
26. Krymskii GF. *Sov. Phys. Dokl.* 22:327 (1977)
27. Bell AR. *Mon. Not. R. Astron. Soc.* 182:147 (1978)
28. Blandford RD, Ostriker JP. *Astrophys. J.* 221:L29 (1978)
29. Jokipii JR. *Astrophys. J.* 146:480 (1966)
30. Jokipii JR, Parker EN. *Astrophys. J.* 155:799 (1969)
31. Lee MA, Volk HJ. *Astrophys. Space Sci.* 24:31 (1973)
32. Cowsik RC, Wilson LW. In *Proceedings of the 13th International Cosmic Ray Conference*, 1:500. Denver, CO: Denver Univ. (1973)
33. Meneguzzi M. In *Proceedings of the 13th International Cosmic Ray Conference*, 1:378. Denver, CO: Denver Univ. (1973)
34. Meneguzzi M. *Nat. Phys. Sci.* 241:100 (1973)
35. Speller R, Thambyahpillai T, Elliot H. *Nature* 235:25 (1972)
36. Allan HR. *Astrophys. Lett.* 12:237 (1972)
37. Cowsik R, Wilson LW. In *Proceedings of the 14th International Cosmic Ray Conference*, ed. K Pinkau, 2:659. Munich, Ger.: Max Planck Inst. Extraterr. Phys. (1975)
38. Lachièze-Rey M, Cesarsky CJ. In *Proceedings of the 14th International Cosmic Ray Conference*, ed. K Pinkau, 2:489. Munich, Ger.: Max Planck Inst. Extraterr. Phys. (1975)
39. Aguilar M, et al. (AMS Collab.) *Phys. Rev. Lett.* 113:121102 (2014)
40. Aguilar M, et al. (AMS Collab.) *Phys. Rev. Lett.* 114:171103 (2015)
41. AMS Collab. "*AMS days at CERN*" *and latest results*. **http://www.ams02.org/2015/04/ams-days-at-cern-and-latest-results-from-the-ams-experiment-on-the-international-space-station/** (2015)
42. Adriani O, et al. *Phys. Rev. Lett.* 105:121101 (2010)
43. Abe K. *Phys. Lett. B* 670:103 (2008)
44. Oliva A. *AMS results on light nuclei: measurement of the cosmic rays boron-to-carbon ratio with AMS-02*. Presented at AMS Days, CERN, Geneva. **https://indico.cern.ch/event/381134/contribution/23/material/slides/0.pdf** (2015)
45. Engelmann JJ, et al. *Astron. Astrophys.* 233:96 (1990)
46. Dwyer R, Meyer P. *Astrophys. J.* 322:981 (1987)
47. Obermeier A, et al. *Astrophys. J.* 742:14 (2011)

48. Muller D, et al. *Astrophys. J.* 374:356 (1991)
49. Ahn HS, et al. *Astropart. Phys.* 30:133 (2008)
50. Swordy SP, et al. *Astrophys. J.* 349:625 (1990)
51. Panov AD, et al. (ATIC Collab.) In *Proceedings of the 30th International Cosmic Ray Conference*, ed. R Caballero, et al., 2:3. Mexico City: Univ. Nac. Auton. Mex. (2008)
52. Cowsik R, Burch B. *Phys. Rev. D* 82:023009 (2010)
53. Oort JH. *Bull. Astron. Inst. Neth.* 6:249 (1932)
54. Rubin VC, Ford WK. *Astrophys. J.* 159:379 (1970)
55. Babcock H. *Lick Obs. Bull.* 19:498 (1939)
56. Bosma A. *The distribution and kinematics of neutral hydrogen in spiral galaxies of various morphological types*. PhD thesis, Univ. Groningen, Groningen, Neth. (1978)
57. Rood HJ, Page TL, Kintner EC, King IR. *Astrophys. J.* 175:627 (1972)
58. Cowsik R, McClelland J. *Astrophys. J.* 180:7 (1973)
59. Gerstein SS, Zel'dovich YB. *JETP Lett.* 4:174 (1966)
60. Cowsik R, McClelland J. *Phys. Rev. Lett.* 29:669 (1972)
61. Marx G, Szalay AS. In *Proceedings of the Europhysics Conference on Neutrinos*, ed. A Frenkel, G Marx, 1:191. Budapest: Cent. Res. Inst. Phys. (1972)
62. Lee BW, Weinberg S. *Phys. Rev. Lett.* 39:165 (1977)
63. Steigman G, Dasgupta B, Beacom JF. *Phys. Rev. D* 86:023506 (2012)
64. Ade PAR, et al. (Planck Collab.) arXiv:1502.01589v2 [astro-ph.co] (2015)
65. Spergel DN. *Science* 347:1100 (2015)
66. Deleted in proof
67. Jeans JH. *Mon. Not. R. Astron. Soc.* 82:123 (1922)
68. Oort JH. *Bull. Astron. Inst. Neth.* 4:342 (1932)
69. Schmidt M. *Bull. Astron. Inst. Neth.* 13:15 (1956)
70. Binney J, Dehnen W. *Mon. Not. R. Astron. Soc.* 287:L5 (1997)
71. Kuijken K, Gilmore G. *Astrophys. J. Lett.* 367:L9 (1991)
72. Bachall JN, Flynn C, Gould A. *Astrophys. J.* 389:234 (1992)
73. Weber W, de Boer W. *Astron. Astrophys.* 509:A25 (2010)
74. McMillan PJ. *Mon. Not. R. Astron. Soc.* 414:2446 (2011)
75. Springel V. *Nature* 435:629 (2005)
76. Navarro JF, Frenk CS, White SDM. *Astrophys. J.* 462:563 (1996)
77. Binney J, Tremaine S. *Galactic Dynamics*. Princeton, NJ: Princeton Univ. Press (1987)
78. Cowsik R, Ratnam C, Bhattacharjee P. *Phys. Rev. Lett.* 76:3886 (1996)
79. Chaudhury S, Bhattacharjee P, Cowsik R. *J. Cosmol. Astropart. Phys.* 090:020 (2010)
80. Burch B, Cowsik R. *Astrophys. J.* 779:35 (2014)
81. Moskalenko IV, Strong AW. *Astrophys. J.* 493:694 (1998)
82. Luca M, Evoli C, Gaggero D, Grasso D. *DRAGON: galactic cosmic ray diffusion code*. Astrophys. Source Code Libr. rec. ascl:1106.011. **http://ascl.net/1106.011** (2011)
83. Parker EN. *Planet. Space Sci.* 13:9 (1965)
84. Parker EN. *Planet. Space Sci.* 14:371 (1966)
85. Gleeson LJ, Axford WI. *Astrophys. J. Lett.* 149:L115 (1969)
86. Trotta R, et al. *Astrophys. J.* 729:106 (2011)
87. Kappl A, Winkler MW. *J. Cosmol. Astropart. Phys.* 09:051 (2014)
88. Mertsch P, Sarkar S. *Phys. Rev. Lett.* 103:081104 (2009)
89. Serpico PD. *Astropart. Phys.* 39:2 (2012)
90. Blasi P. *Phys. Rev. Lett.* 103:051104 (2009)
91. Fujita Y, Kohri K, Yamazaki R, Ioka K. *Phys. Rev. D* 80:063003 (2009)
92. Mertsch P, Sarkar S. *Phys. Rev. D* 90:061301 (2014)
93. Blasi P, Serpico PD. *Phys. Rev. Lett.* 103:081103 (2009)
94. Berezhko EG, Ksenofontov LT. *J. Phys. Conf. Ser.* 409:012025 (2013)
95. Kachelreiss M, Neronov A, Semikoz DV. *Phys. Rev. Lett.* 115:181103 (2015)
96. Yuksel H, Kistler MD, Stanev T. *Phys. Rev. Lett.* 103:051101 (2009)

97. Profumo S. *Cent. Eur. J. Phys.* 10:1 (2012)
98. Hooper D, Blasi P, Dario SP. *J. Cosmol. Astropart. Phys.* 01:025 (2009)
99. Cowsik R. *Astrophys. J.* 241:1195 (1980)
100. Eichler D. *Astrophys. J.* 237:809 (1980)
101. Cholis I, Hooper D. *Phys. Rev. D* 89:043013 (2014)
102. Shaviv NJ, Nakar E, Piran T. *Phys. Rev. Lett.* 103:111302 (2009)
103. Gaggero D, et al. *Phys. Rev. Lett.* 111:021102 (2013)
104. Yuan Q, et al. arXiv:1304.1482v3 [astro-ph.HE] (2014)
105. Cowsik R, Lee MA. *Astrophys. J.* 228:297 (1979)
106. Nishimura J, Kobayashi T, Komori Y, Yoshida K. *Adv. Space Res.* 19:767 (1997)
107. Israel MH. *Braz. J. Phys.* 44:530 (2014)
108. Katz B, Blum K, Morag J, Waxman E. *Mon. Not. R. Astron. Soc.* 405:1458 (2010)
109. Blum K, Katz B, Waxman E. arXiv:1305.1324 [astro-ph.HE] (2013)
110. Kruskal M, Ahlen SP, Tarlé G. arXiv:1410.7239v6 [astro-ph.HE] (2016)
111. Bringmann T, Salati P. *Phys. Rev. D* 75:083006 (2007)
112. Cowsik R, Burch B, Madziwa-Nussinov T. *Astrophys. J.* 786:124 (2014)
113. Cowsik R, Burch B, Madziwa-Nussinov T. arXiv:1505.00305v2 [astro-ph.HE] (2015)
114. Cowsik R, Madziwa-Nussinov T. *Proc. Sci.* ICRC2015:548 (2015)
115. Chapell JH, Webber WR. In *Proceedings of the 17th International Cosmic Ray Conference* (*ICRC17*), 9:97. Gif-sur-Yvette, France: Cent. Étud. Nucl. Saclay (1981)
116. Blasi P, et al. *Astrophys. J.* 755:121 (2012)
117. Schure KM, Bell AR, Drury LO, Bykov AM. *Space Sci. Rev.* 173:491 (2012)
118. Bell AR. *Mon. Not. R. Astron. Soc.* 442:2224 (2015)
119. Ellison DC. *Am. Inst. Phys.* 1516:195 (2013)
120. Chevalier RA, Fransson C. *Lect. Notes Phys.* 598:171 (2003)
121. Binns WR. *Science* 334:1071 (2011)
122. Telezhinksy I, Dwarkadas VV, Pohl M. *Astron. Astrophys.* 541:A153 (2012)
123. Ackermann M, et al. *Science* 334:1103 (2011)
124. Potgieter M. *Living Rev. Solar Phys.* 10:3 (2013)
125. Acero F, et al. *Astrophys. J. Suppl.* 218:23 (2015)
126. Armstrong JW, Rickett BJ, Spangler SR. *Astrophys. J.* 443:209 (1995)
127. Lewandowski W, Dembska M, Kijak J, Kowalińska M. *Mon. Not. R. Astron. Soc.* 434:69 (2013)
128. Torii S. (CALET Collab.) *Proc. Sci.* ICRC2015:581 (2015)
129. Seo FS, et al. *Adv. Space Res.* 53:1451 (2014)
130. di Mauro M, Donato F, Goudelis A, Serpico PD. *Phys. Rev. D* 90:085017 (2014)
131. Duperray RP, Huang C-Y, Protasov KV, Buénerd M. *Phys. Rev. D* 68:094017 (2003)
132. Simon M, Molnar A, Roesler S. *Astrophys. J.* 499:250 (1998)
133. Gaisser TK, Schaefer RK. *Astrophys. J.* 394:174 (1992)
134. Tan L, Ng L. *Phys. Rev. D* 26:1179 (1982)
135. Stephens SA. *Astrophys. Space Sci.* 76:87 (1981)
136. Strong AW, Moskalenko IV. *Astrophys. J.* 509:212 (1998)
137. Gunn JE, et al. *Astrophys. J.* 223:1015 (1978)
138. Stecker FW. *Astrophys. J.* 223:1032 (1978)
139. Jungman G, Kamionkowski M, Griest K. *Phys. Rep.* 267:195 (1996)
140. Bertone G, Hooper D, Silk J. *Phys. Rep.* 405:279 (2005)
141. Bergstrom L. *Ann. Phys.* 524:479 (2012)
142. Ibarra A, Tran D, Weniger C. *Int. J. Mod. Phys. A* 28:1330040 (2013)
143. Cirelli M, et al. arXiv:1012.4515v4 [hep-ph] (2012)
144. Ackermann M, et al. *Phys. Rev. Lett.* 115:231301 (2015)
145. Abazajian KN. *J. Cosmol. Astropart. Phys.* 01:041 (2012)
146. Kamionkowski M, Koushiappas SM. arXiv:0801.3269v2 [astro-ph] (2008)
147. Nierop SCA. *The Sommerfeld enhancement*. PhD thesis, Fac. Math. Nat. Sci., Univ. Groningen, Groningen, Neth. (2009)

148. Evoli C, et al. arXiv:1108.0664v2 [astro-ph.HE] (2012)
149. Bergstrom L, et al. *Phys. Rev. Lett.* 111:171101 (2013)
150. Conrad J. arXiv:1411.1925v1 [hep-ph] (2014)
151. Jin H-B, Wu Y-L, Zhou Y-F. arXiv:1504.04604v3 [hep-ph] (2015)
152. Giesen G, et al. *J. Cosmol. Astropart. Phys.* 09:023 (2015)
153. Hamaguchi K, Moroi T, Nakayama K. *Phys. Lett. B* 747:523 (2015)
154. Adriani O, et al. *Phys. Rev. Lett.* 111:081102 (2013)

Annual Review of Nuclear and Particle Science

Volume 66, 2016

Contents

Errata

An online log of corrections to *Annual Review of Nuclear and Particle Science* articles may be found at http://www.annualreviews.org/errata/nucl